GRADIENT FLOW BROADBAND BEAMFORMING AND SOURCE SEPARATION

Milutin Stanacevic, Gert Cauwenberghs[*]

ECE Dept. and CLSP
Johns Hopkins University
Baltimore, MD 21218
{miki,gert}@jhu.edu

George Zweig

RLE, MIT, Cambridge, MA 02139;
LANL, Los Alamos, NM 87545
gzweig@mit.edu

ABSTRACT

We present and demonstrate a method for blind separation and bearing estimation of broadband traveling waves, impinging on a sensor array with dimensions smaller than the shortest wavelength in the sources. By sensing spatial and temporal gradients of the received signal, the problem of separating mixtures of time-delayed sources reduces to that of separating instantaneous mixtures of the gradient components of the sources using conventional tools of independent component analysis. Experimental results demonstrate real-world separation of speech in outdoors and indoors environments, using a planar array of four microphones within a 5 mm radius and analog circuits computing spatial and temporal derivatives.

1. INTRODUCTION

Blind separation of real-world acoustic sources is generally considered a hard and unsolved problem, with mixed degree of success in practical realizations. Closely linked to acoustic source separation is the problem of source localization, or bearing angle estimation. Super-resolution spectral methods are commonly used to localize multiple narrowband sources [1], yet little is known about the problem of localizing and separating multiple broadband sources.

Because of the wave properties of sound, it appears that instantaneous mixing models as standardly used in independent component analysis would be inadequate. The conventional approach is to blindly estimate multiple time delays in the wave propagation between sources and microphones, besides blindly estimating the sources themselves [2, 3, 4]. Several systems based on this approach have been demonstrated on real speech, *e.g.,* [5, 6, 7, 8, 9, 10].

Like optical flow for motion estimation [11], the direction of sound propagation can be inferred directly from sensing spatial and temporal gradients of the wave signal, on a sub-wavelength scale. This principle is exploited in biology [12], and implemented in biomimetic MEMS systems [13]. Wavefront sensing in space for localizing sound has been in practice since the pioneering work by Blumlein in the 1930s [14], a precursor to the advances in binaural signal processing that we know today.

Gradient flow converts the problem of separating delayed mixtures into a simpler problem of separating instantaneous mixtures of spatial and temporal gradients of the wave signals. This formulation is equivalent to that of standard ICA, and a number of approaches exist for such blind separation, some utilizing VLSI hardware [15]. The mixing coefficients obtained from ICA directly yield the angles of the incoming waves. Therefore our method can be seen as a broadband beamforming extension to static ICA, performing at once blind separation *and* localization of traveling waves.

In what follows we review the principle of operation, and present experimental results that demonstrate real-world separation and localization of speech sources using a planar geometry of miniature microphones (Knowles IM-3268) on a spatial scale significantly smaller than the shortest wavelength present in the speech. Details of theoretical nature are given in a precursor of this paper [16].

2. MODELS

We consider linear mixtures of traveling waves emitted by sources at various locations, and observed over a distribution of sensors in space. The distribution of sensors could be continuous or discrete. In what follows we assume an array of discrete sensors, but the theory applies as well to sensors distributed continuously in space. However, the sources are assumed to be discrete.

2.1. Instantaneous Series Expansion

Let the coordinate system $\mathbf{r}$ be centered in the array so that the origin coincides with the "center of mass" of the sensor distribution. We define $\tau(\mathbf{r})$ as the time lag between the wavefront at point $\mathbf{r}$ and the wavefront at the center of the array, *i.e.,* the propagation time $\tau(\mathbf{r})$ is referenced to the center of the array. Then the field $s(t + \tau(\mathbf{r}))$ can be expanded about the center of the array in the power series

[*]This work was partly supported by ONR N00014-99-1-0612, ONR/DARPA N00014-00-C-0315 and N00014-00-1-0838, and NSF MIP-9702346.

expansion,

$$s(t+\tau(\mathbf{r})) = s(t) + \tau(\mathbf{r})\dot{s}(t) + \tfrac{1}{2}\tau(\mathbf{r})^2\ddot{s}(t) + \dots \quad (1)$$

The ratio in amplitude of successive terms in the series should not be too large so that it converges properly, nor too small so an adequate number of terms can be resolved to identify the sources. This implies that the dimensions of the sensor array should be smaller than that of the (largest) wavelength, but not much smaller. More details on the *wave-resolution* conditions are given in [16].

2.2. The far field

In the *far-field* approximation, the distance from the source is much larger than the dimensions of the sensor array. This is a sensible approximation for an integrated MEMS or VLSI array with dimensions typically smaller than 1 cm. Then the wavefront delay $\tau(\mathbf{r})$ is approximately linear in the projection of $\mathbf{r}$ on the unit vector $\mathbf{u}$ pointing towards the source,

$$\tau(\mathbf{r}) \approx \frac{1}{c}\mathbf{r}\cdot\mathbf{u} \quad (2)$$

where c is the speed of (acoustic or electromagnetic) wave propagation.

2.3. Signal Model

We assume that the sources are statistically independent so that their joint probability density function factors:

$$\Pr(\mathbf{s}) = \prod_{\ell=1}^{\mathcal{L}} \varphi^\ell(s^\ell). \quad (3)$$

This allows us to apply ICA to the instantaneous mixture problem that follows.

2.4. Mixing and Acquisition Model

Let $x(\mathbf{r},t)$ be the signal mixture picked up by a sensor at position $\mathbf{r}$. As one special case we will consider a two-dimensional array of sensors, with position coordinates p and q so that $\mathbf{r}_{pq} = p\mathbf{r}_1 + q\mathbf{r}_2$ with orthogonal vectors $\mathbf{r}_1$ and $\mathbf{r}_2$ in the sensor plane.

In the *far-field* approximation (2), each source signal s^ℓ contributing to x_{pq} is advanced in time by $\tau_{pq}^\ell = p\tau_1^\ell + q\tau_2^\ell$, where

$$\begin{aligned}\tau_1^\ell &= \frac{1}{c}\mathbf{r}_1\cdot\mathbf{u}^\ell \\ \tau_2^\ell &= \frac{1}{c}\mathbf{r}_2\cdot\mathbf{u}^\ell \end{aligned} \quad (4)$$

are the inter-time differences (ITD) of source ℓ between adjacent sensors on the grid along the p and q place coordinates, respectively. Knowledge of the *angle coordinates* τ_1^ℓ and τ_2^ℓ uniquely determines, through (4), the direction vector $\mathbf{u}^\ell$ along which source s^ℓ impinges the array, in reference to the $\{p,q\}$ plane[1].

The series expansion (1) for each source yields

$$x_{pq}(t) = \sum_{\ell=1}^{\mathcal{L}} s^\ell(t) + \tau_{pq}^\ell\dot{s}^\ell(t) + \tfrac{1}{2}(\tau_{pq}^\ell)^2\ddot{s}^\ell(t) + \dots + n_{pq}(t) \quad (5)$$

where $n_{pq}(t)$ represents additive noise in the sensor observations. Although not essential, we will assume that the observation noise is independent across sensors, and follows a univariate Gaussian distribution $n_{pq}(t) \propto \mathcal{N}(0,\sigma)$.

In what follows we will concentrate on the first two terms in the series expansion (5), linear in the space coordinates:

$$x_{pq}(t) \approx \sum_{\ell=1}^{\mathcal{L}} s^\ell(t) + (p\tau_1^\ell + q\tau_2^\ell)\dot{s}^\ell(t) + n_{pq}(t)\,. \quad (6)$$

3. GRADIENT FLOW ICA

A gradient flow formulation is obtained by isolating time derivatives of the linearly combined signals by taking spatial gradients of x along p and q. The advantage of this technique is that it effectively reduces the problem of estimating $s^\ell(t)$ and τ_i^ℓ to that of separating instantaneous mixtures of gradient components of the independent source signals.

For array dimensions smaller than but comparable to the largest wavelength (*wave-resolving* conditions [16]), individual terms in the series expansion (5) can be resolved. Different linear combinations[2] of the signals s^l are thus obtained by taking spatial derivatives of various orders i and j along the position coordinates p and q, around the origin $p=q=0$:

$$\begin{aligned}\xi_{ij}(t) &\equiv \left.\frac{\partial^{i+j}}{\partial^i p\,\partial^j q}x_{pq}(t)\right|_{p=q=0} \\ &= \sum_\ell (\tau_1^\ell)^i(\tau_2^\ell)^j\,\frac{d^{i+j}}{d^{i+j}t}s^\ell(t) \;+\; \nu_{ij}(t), \end{aligned} \quad (7)$$

where ν_{ij} are the corresponding spatial derivatives of the sensor noise n_{pq} around the center. The point here is that all signals s^l in (7) are differentiated to the *same* order $i+j$ in time. Therefore, taking spatial derivatives ξ_{ij} of order $i+j \le k$, and differentiating ξ_{ij} to order $k-(i+j)$ in time yields a number of different linear observations in the kth-order time derivatives of the signals s^ℓ.

[1] We assume that the sources impinge on top, not on bottom, of the array. This is a reasonable assumption for an integrated MEMS or VLSI array since the substrate masks any source impinging from beneath.

[2] The issue of linear independence will be revisited when we consider the geometry of the source angles relative to that of the sensors in Section 3.1.

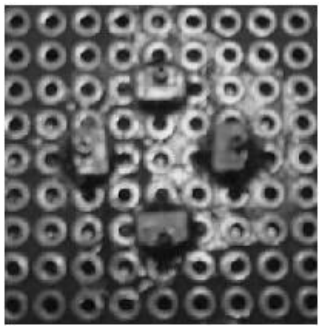

Fig. 1. *Geometry of four co-planar sensors computing first-order gradient flow in two dimensions according to (9). Using four Knowles IM-3268 microphones, the array is contained within a 5 mm radius.*

As an example, consider the first-order case $k = 1$, corresponding to (6):

$$\begin{aligned} \xi_{00}(t) &= \textstyle\sum_\ell s^\ell(t) + \nu_{00}(t), \\ \xi_{10}(t) &= \textstyle\sum_\ell \tau_1^\ell \dot{s}^\ell(t) + \nu_{10}(t), \\ \xi_{01}(t) &= \textstyle\sum_\ell \tau_2^\ell \dot{s}^\ell(t) + \nu_{01}(t). \end{aligned} \tag{8}$$

Estimates of ξ_{00}, ξ_{10} and ξ_{01} are obtained with just four sensors x_{pq}:

$$\begin{aligned} \xi_{00} &\approx \tfrac{1}{4}\big(x_{-1,0} + x_{1,0} + x_{0,-1} + x_{0,1}\big) \\ \xi_{10} &\approx \tfrac{1}{2}\big(x_{1,0} - x_{-1,0}\big) \\ \xi_{01} &\approx \tfrac{1}{2}\big(x_{0,1} - x_{0,-1}\big) \end{aligned} \tag{9}$$

A practical realization of this configuration, using miniature microphones, is illustrated in Figure 1. Taking the time derivative of ξ_{00}, we thus obtain from the sensors a linear instantaneous mixture of the time-differentiated source signals,

$$\begin{bmatrix} \dot{\xi}_{00} \\ \xi_{10} \\ \xi_{01} \end{bmatrix} \approx \begin{bmatrix} 1 & \cdots & 1 \\ \tau_1^1 & \cdots & \tau_1^{\mathcal{L}} \\ \tau_2^1 & \cdots & \tau_2^{\mathcal{L}} \end{bmatrix} \begin{bmatrix} \dot{s}^1 \\ \vdots \\ \dot{s}^{\mathcal{L}} \end{bmatrix} + \begin{bmatrix} \dot{\nu}_{00} \\ \nu_{10} \\ \nu_{01} \end{bmatrix}, \tag{10}$$

an equation in the standard form $\mathbf{x} = \mathbf{A}\mathbf{s} + \mathbf{n}$, where $\mathbf{x}$ is given and the mixing matrix $\mathbf{A}$ and sources $\mathbf{s}$ are unknown. Ignoring for now the noise term $\mathbf{n}$ (and for a square matrix, $\mathcal{L} = 3$) this problem setting is standard in ICA, with an independence assumption (3) on the sources $\mathbf{s}$. ICA produces, at best, an estimate $\hat{\mathbf{s}}$ that recovers the original sources $\mathbf{s}$ up to arbitrary scaling and permutation. The direction cosines τ_i^ℓ are found from the ICA estimate of $\mathbf{A}$, after first normalizing each column (*i.e.,* , each source estimate) so that the first row of the estimate $\hat{\mathbf{A}}$, like the real $\mathbf{A}$ according to (10), contains all ones. This simple procedure together with (4) yields estimates of the direction vectors $\hat{\mathbf{u}}^\ell$ along

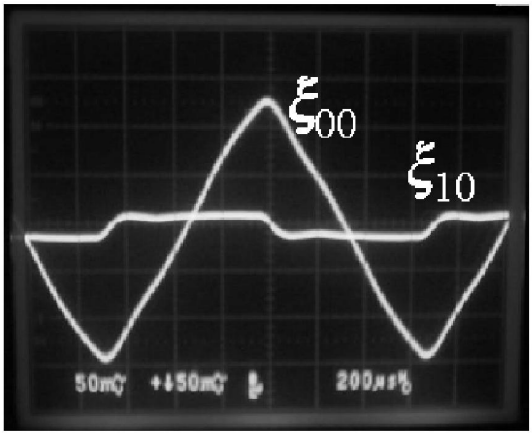

Fig. 2. *Common-mode ξ_{00} and gradient ξ_{10} components obtained from the microphone array of Fig. 1, for a single audio signal generated from a triangular waveform source. ξ_{10} approximates the time derivative $\dot{\xi}_{00}$, scaled by the angle cosine τ_1 in all four quadrants.*

with the source estimates $\hat{s}^\ell(t)$, which are obtained by integrating the components of $\hat{\mathbf{s}}$ over time and removing the DC components.

It is interesting to note the functional similarity between (10), with $\mathcal{L} = 1$, and *optical flow* for constraint-solving velocity estimation in a visual scene [11]. Figure 2 illustrates the temporal derivative relationship between common-mode ξ_{00} and differential ξ_{10} components of the array outputs, of which the relative amplitude reveals one cosine of the angle of incidence.

3.1. Noise Characteristics

The presence of the noise term $\mathbf{n}$ complicates the estimation of $\mathbf{s}$ and $\mathbf{A}$. For localization of a *single* source, simple expressions can be obtained for the Cramer-Rao lower bound on the variance of the τ_i estimates, assuming second-order (Gaussian) statistics. As in [17], this bound depends on the aperture, *i.e.,* the dimensions of the array relative to one wavelength. For miniature arrays, it is therefore important to boost the signal to noise ratio to compensate for the loss in aperture. The critical factor here is a high sensitivity of gradient acquisition, which can be attained by a differential sensor design either through mechanical coupling [12, 13] or differential amplification at the sensor level.

Cramer-Rao bounds on ${\tau_i}^\ell$ for joint localization and separation are harder to come by, since it requires assumptions on the higher-order statistics of the signals. Still, we can infer noise properties of the estimated sources $\hat{s}$ assuming fixed values for ${\tau_i}^\ell$. Assume a standard formulation of ICA (*e.g.,* [3]) that attempts to linearly unmix the observations $\mathbf{x}$:

$$\hat{\mathbf{s}} = \hat{\mathbf{A}}^{-1}\mathbf{x} = \hat{\mathbf{A}}^{-1}\mathbf{A}\mathbf{s} - \hat{\mathbf{A}}^{-1}\mathbf{n}, \tag{11}$$

where $\mathbf{A}$ is square and invertible. Assume also a reasonable ICA estimate $\hat{\mathbf{A}}$ so that (11) reduces to $\hat{\mathbf{s}} \approx \mathbf{s} - \mathbf{A}^{-1}\mathbf{n}$, disregarding arbitrary permutation and scaling in the source estimates. The error term $\mathbf{e} \equiv -\mathbf{A}^{-1}\mathbf{n}$ contributes *variance* to the estimate $\hat{\mathbf{s}}$; in general the noise $\mathbf{n}$ will also affect the estimate $\hat{\mathbf{A}}$ and produce a *bias* term in $\hat{\mathbf{s}}$ according to (11).

The functional form of the error $\mathbf{e}$ allows us to estimate the noise characteristics of the source estimates, without considering details on how ICA obtained these estimates. The covariance of the estimation error is

$$E[\mathbf{e}\mathbf{e}^T] = \mathbf{A}^{-1}E[\mathbf{n}\mathbf{n}^T](\mathbf{A}^{-1})^T. \qquad (12)$$

In other words, the error covariance depends on the covariance of the sensor noise, the geometry of the sensor array, and the orientation of the sources $\mathbf{u}^\ell$ as determined by the mixing matrix $\mathbf{A}$.

For example, consider the case $k = 1$, suitable for a miniature array. $\mathbf{A}$ in (10) is square when $\mathcal{L} = 3$. The determinant of $\mathbf{A}$ can be geometrically interpreted as the volume of the polyhedron spanned by the three source direction vectors $\mathbf{u}^\ell$. The error covariance is minimum when the vectors are orthogonal, and the estimates of $\mathbf{s}$ and $\mathbf{A}$ become unreliable as the source direction vectors $\mathbf{u}^\ell$ approach the same plane. Therefore, to first order ($k = 1$) at most three *non-coplanar* sources can be separated and localized with a planar array of sensors.

Arrays of larger dimensions support a larger number of terms k, and thus a larger number of sources $\mathcal{L}$, given by the number of mixture observations up to order k in (7). The condition that $\mathbf{A}$ as determined by (7) be full rank amounts to constraints on the geometry of the source direction vectors $\mathbf{u}^l$. For instance, only one source can lie along any given direction $\mathbf{u}$.

When the number of sources present is greater than the number of gradient observations $\ell_{\max}$ in (7), separation and localization is still possible, but requires an informative *prior* on the sources (3). In particular, a sparse ICA decomposition is obtained in the overcomplete case $\mathcal{L} > \ell_{\max}$ by using a Laplacian prior on the sources [18]. For example, overcomplete ICA could be directly applied on the mixture (10) to separate more than three *sparse* sources.

4. EXPERIMENTAL SETUP AND RESULTS

To demonstrate source separation and localization in a real environment, we used the experimental setup of Figure 1, with four omnidirectional miniature microphones (Knowles IM-3268) as specified by (9) with radius $|\mathbf{r}_1| = |\mathbf{r}_2| = 1$ cm. Continuous-time estimates of common-mode component ξ_{00}, spatial gradients ξ_{10} and ξ_{01}, and time derivative $\dot{\xi}_{00}$ are obtained using analog circuits shown in Figure 3. The time derivative $\dot{\xi}_{00}$ is constructed by feeding ξ_{00} through a high-pass filter with 20 kHz cut-off frequency. Signals ξ_{10} and ξ_{01} are amplified to obtain larger dynamic range and thus

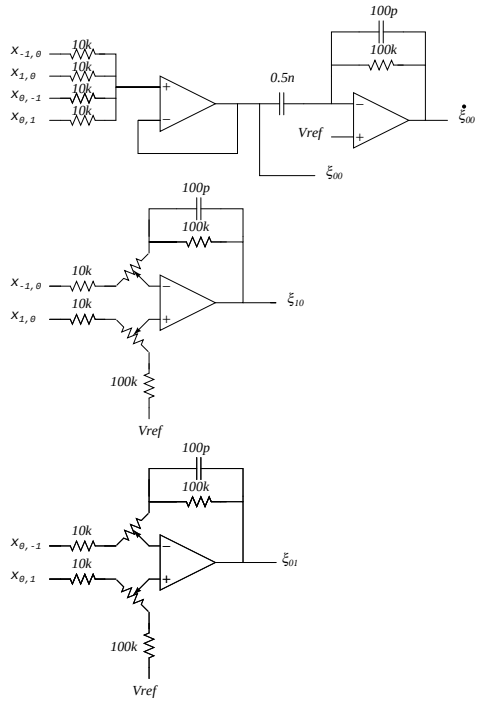

Fig. 3. *Analog circuit computing common-mode ξ_{00}, spatial derivatives ξ_{10} and ξ_{01}, and the common-mode time derivative $\dot{\xi}_{00}$*

larger higher signal-to-noise (SNR) ratio, where the reference voltage V_{ref} is chosen in the middle of the operating voltage range. The signals $\dot{\xi}_{00}$, ξ_{10} and ξ_{01} are fed through anti-alias low-pass filters with 8 kHz cut-off frequency and digitized to 16-bit precision at 16 kHz sampling rate, over a five second time window.

Differences in gain between opposing microphones due to mismatch contributes a common-mode component in the estimated gradients ξ_{10} and ξ_{01}. This component deteriorates separation performance and needs to be minimized. Weighted subtraction, realized using the potentiometers in Figure 3, is implemented to calibrate for mismatch. In addition, an LMS adaptive filter is applied on the digitized signals to further reduce the common-mode component ξ_{00} present in ξ_{10} and ξ_{01}, prior to applying linear instantaneous (fast) ICA.

We conducted experiments in two distinct environments: outdoors surrounded by buildings at a 30 m distance in the presence of wind and other ambient noise, and indoors in a reverberant room with dimensions 8, 4, and 2.7 m with office furniture. Two male speakers were both 50cm from the microphone array and from each other. The digitized analog signals ξ_{00}, ξ_{10}, ξ_{01}, $\dot{\xi}_{00}$, along with the reconstructed sources $\hat{s}_1$ and $\hat{s}_2$, are shown in Figures 4 and 5. Listening tests and visual inspection of the waveforms reveals that the cross-talk in the unmixed signals $\hat{s}_1$ and $\hat{s}_2$ is less than -20 dB for the outdoors environment, and -12 dB for the in-

doors environment. This performance is adequate for most hearing aids applications. The indoors performance is remarkable given that the model assumes planar wave signals without reverberation.

5. CONCLUDING REMARKS

A method for localizing and separating broadband sources in space, by measuring spatial and temporal gradients of the field over a sensor array or distributed sensor, and then performing instantaneous ICA separation, has been described. The ICA solution yields estimates of the sources, along with the cosines of the angles of the sources with respect to the coordinate axes of the array. Three independent and non-coplanar sources can be extracted with as few as four planar sensors.

The main limiting assumption is that the sources propagate as planar waves, although in practice we demonstrated the method to work reasonably well even under severe multipath conditions. For further improvements in performance, deconvolutive ICA [7] could perform a multi-path decomposition yielding angles of incidence for each of the propagation paths. In principle these could be used to identify the absolute position of the source in the environment, or possibly the environment itself.

Conventional wisdom dictates that large sensor arrays should be used for source separation and beamforming to warrant sufficient spatial diversity across sensors. We have shown and experimentally demonstrated that a miniature gradient sensor of dimensions smaller than the shortest wavelength in the sources gives results comparable to the best experimental results available with larger arrays. Surely the noise performance deteriorates with shrinking aperture, but this can be compensated for with improved sensors that are highly sensitive to gradients with large common-mode rejection. Since smaller is better for many applications, we believe that the largest gains can be gotten by focusing on the design and development of gradient sensitive sensors, *e.g.*, using MEMS [13] technology. Hearing aids and cell phones would be just a few of the applications to benefit dramatically from such developments.

6. REFERENCES

[1] S. Haykin, *Adaptive Filter Theory*, Prentice-Hall, 2nd edition, 1991.

[2] S. Li and T. Sejnowski, "Adaptive separation of mixed broadband sound sources with delays by a beamforming herault-jutten network," *IEEE J. Oceanic Eng.*, vol. 20, no. 1, pp. 73–79, Jan. 1995.

[3] A.J. Bell and T.J. Sejnowski, "An information maximization approach to blind separation and blind deconvolution," *Neural Computation*, vol. 7, no. 6, pp. 1129–1159, Nov 1995.

[4] K. Torkkola, "Blind separation of delayed sources based on information maximization," in *Proc. IEEE Int. Conf. Acoustics, Speech and Signal Processing (ICASSP'96)*, Atlanta GA, 1996.

[5] J.L. Flanagan, D.A. Berkley, G.W. Elko, J.E. West, and M.M. Sondhi, "Autodirective microphone systems," *ACUSTICA*, vol. 73, no. 1, pp. 58–91, 1991.

[6] G. Elko and A. Pong, "A steerable and variable first-order differential microphone array," in *Proc. IEEE Int. Conf. on Acoustics, Speech and Signal Processing (ICASSP'97)*, Munich, Germany, April 1997, pp. 223–226.

[7] T-W. Lee, A. Bell, and R. Orglmeister, "Blind source separation of real world signals," in *Proceedings of International Conference on Neural Networks*, Houston, 1997.

[8] L. Parra and C. Spence, "Convolutive blind separation of non-stationary sources," *IEEE Transactions Speech and Audio Processing*, pp. 320–327, 2000.

[9] M. Brandstein and H. Silverman, "A practical methodology for speech source localization with microphone arrays," *Computer, Speech and Language*, vol. 11, no. 2, pp. 91–126, 1997.

[10] S. Affes and Y. Granier, "A signal subspace tracking algorithm for microphone array processing of speech," *IEEE Trans. Speech and Audio Processing*, vol. 5, no. 5, pp. 425–437, 1997.

[11] J.L. Barron, D.J. Fleet, and S.S. Beauchemin, "Performance of optical flow techniques," *International Journal of Computer Vision*, vol. 12, no. 1, pp. 43–77, 1994.

[12] D. Robert, R.N. Miles, and R.R. Hoy, "Tympanal hearing in the sarcophagid parasitoid fly emblemasoma sp.: the biomechanics of directional hearing," *J. Experimental Biology*, vol. 202, pp. 1865–1876, 1999.

[13] A.G. Andreou, D.H. Goldberg, E. Culurciello, M. Stanacevic, and G. Cauwenberghs, "Heterogeneous integration of biomimetic acoustic microsystems," in *Proc. IEEE Int. Symp. Circuits and Systems (ISCAS'2001)*, Sydney, Australia, May 6-9 2001.

[14] A.D. Blumlein, "Improvements in and relating to sound-transmission, sound-recording and sound-reproducing systems," *British Patent*, , no. 394325, 1933.

[15] M.H. Cohen and A.G. Andreou, "Current-mode subthreshold mos implementation of herault-jutten autoadaptive network," *IEEE J. Solid-State Circuits*, vol. 27, pp. 714–727, May 1992.

[16] G. Cauwenberghs, M. Stanacevic, and G.Zweig, "Blind broadband source localization and separation in miniature sensor arrays," in *Proc. IEEE Int. Symp. Circuits and Systems (ISCAS'2001)*, Sydney, Australia, 2001, vol. 3, pp. 193 –196.

[17] B. Friedlander, "On the cramer-rao bound for time delay and doppler estimation," *IEEE Transactions on Information Theory*, vol. 30, no. 3, pp. 575–580, 1984.

[18] M.S. Lewicki and T.J. Sejnowski, "Learning overcomplete representations," *Neural Computation*, vol. 12, pp. 337–365, 2000.

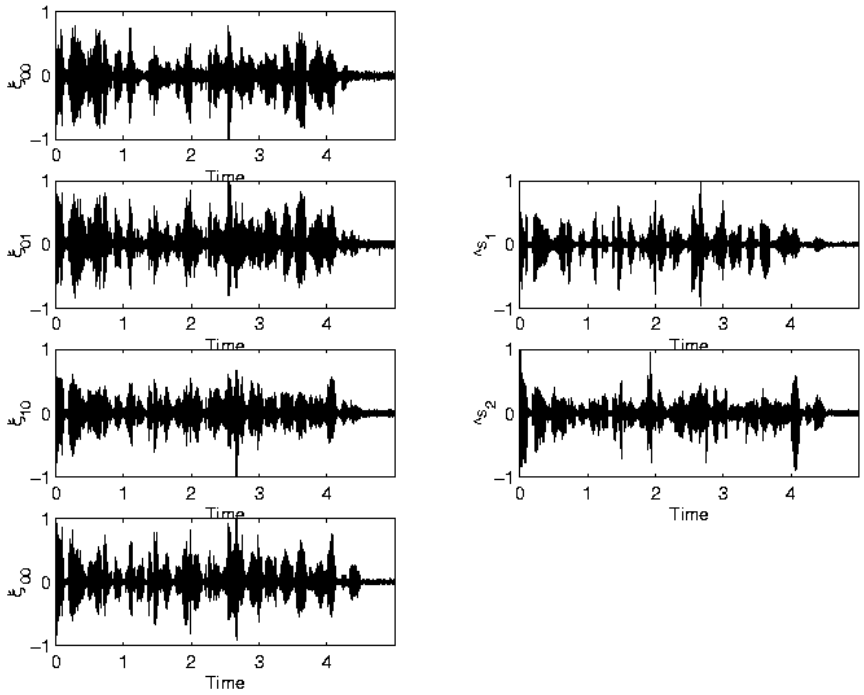

Fig. 4. *Experimental separation of speech from two male speakers in an outdoors setting.* Left: *Measured components* ξ_{00}, ξ_{10}, ξ_{01} *and its time derivative* $\dot{\xi}_{00}$, *produced by the analog circuit in Fig. 3 on outputs from the microphone array in Fig. 1.* Right: *Reconstructed sources* $\hat{s}_1$ *and* $\hat{s}_2$ *using static ICA on* ξ_{10}, ξ_{01} *and* $\dot{\xi}_{00}$.

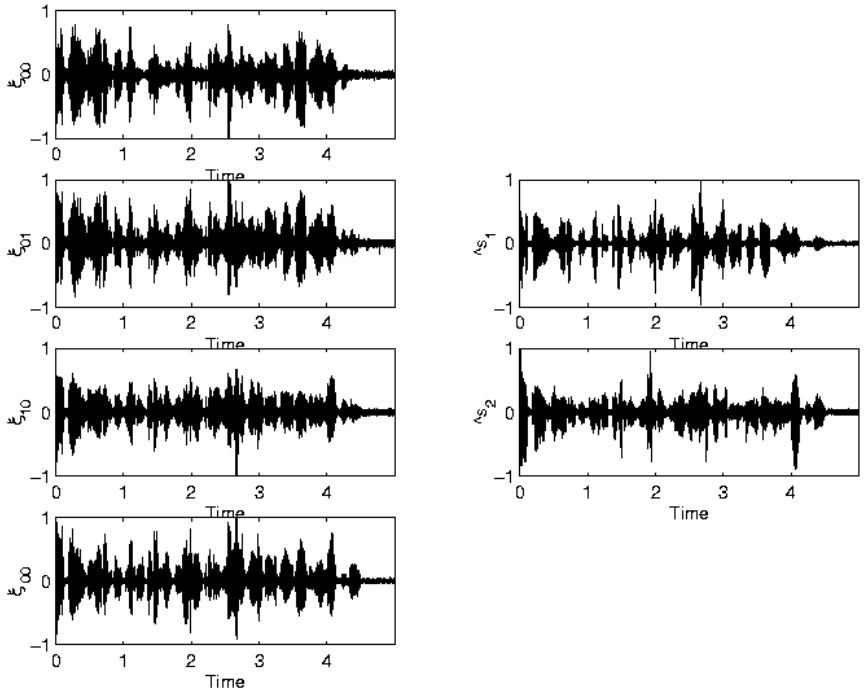

Fig. 5. *Experimental separation of speech from two male speakers in a reverberant indoors setting. Same conditions as in Fig. 4.*